ADVANCED MATERIALS

Supporting Information

for *Adv. Mater.,* DOI: 10.1002/adma.202202188

Large-Scale Integration of a Zinc Metasilicate Interface Layer Guiding Well-Regulated Zn Deposition

Ruiting Guo, Xiong Liu, Fanjie Xia, Yalong Jiang, Huazhang Zhang, Meng Huang, Chaojiang Niu, Jinsong Wu, Yan Zhao, Xuanpeng Wang, Chunhua Han,* and Liqiang Mai**

Supporting Information

Large-Scale Integration of a Zinc Metasilicate Interface Layer Guiding Well-Regulated Zn Deposition

Ruiting Guo, Xiong Liu, Fanjie Xia, Yalong Jiang, Huazhang Zhang, Meng Huang, Chaojiang Niu, Jinsong Wu, Yan Zhao, Xuanpeng Wang, Chunhua Han,* and Liqiang Mai**

R. Guo, F. Xia, Dr. Y. Jiang, Dr. M. Huang, Prof. J. Wu, Prof. Y. Zhao, Prof. C. Han, Prof. L. Mai, State Key Laboratory of Advanced Technology for Materials Synthesis and Processing, Wuhan University of Technology, Wuhan 430070, China

Dr. X. Liu, Prof. C. Niu, School of Materials Science and Engineering, Zhengzhou University, Zhengzhou 450001, China

Dr. H. Zhang, Dr. X. Wang, Department of Physical Science & Technology, School of Science, Wuhan University of Technology, Wuhan 430070, China

Prof. L. Mai, Dr. X. Wang, Foshan Xianhu Laboratory of the Advanced Energy Science and Technology Guangdong Laboratory, Xianhu hydrogen Valley, Foshan 528200, China

Prof. L. Mai, Hubei Longzhong Laboratory, Xiangyang 441000, Hubei, China

E-mail: mlq518@whut.edu.cn; hch5927@whut.edu.cn; liuxiong@zzu.edu.cn

Experimental section

Preparation of Zn@ZSO composite foil. 0.24 g SiO_2 (15±5 nm) nanoparticles were first added into 35 mL deionized water, and the solution was stirred. Then 50 μL 2 M NaOH aqueous solution was added. At this time, the pH of the solution was 10.6. Next, the obtained solution and a piece of 100 μm-thick Zn foil (2.5 cm × 4.5 cm) were transferred into a 50 mL Teflon-lined stainless-steel autoclave. After reacting at 120 °C for 36 h, the Zn foil was taken out and washed with deionized water.

For large-area Zn@ZSO, the additive amounts of SiO_2, NaOH aqueous solution, and deionized water were 3.6 g, 875 μL, and 360 mL, respectively. The Zn foil (100 cm × 10 cm) was rolled and put into a 500 mL Teflon-lined stainless-steel autoclave. The reaction temperature and time are consistent with the above mentioned.

Preparation of Zn@Zn-Ti-O composite foil. 0.04 g TiO_2 (5-10 nm, hydrophobic) nanoparticles

and 50 μL 2 M NaOH aqueous solution were added in 35 mL deionized water one after another. The subsequent process was the same as the preparation of Zn@ZSO foil.

Preparation of $K_{0.27}MnO_2 \cdot 0.54H_2O$. The synthesis of $K_{0.27}MnO_2 \cdot 0.54H_2O$ referred to a previous work[1]. First, 6 g $KMnO_4$ and 10 g D(+)-Glucose were fully dissolved in 100 and 40 mL deionized water, respectively. After adding the former to the later and stirring the mixture for 40 s, a brown gel formed. The gel was then transferred to an oven at 110 °C for 12 h, and a xerogel could be obtained. The xerogel was ground first, and then calcinated at 400 °C for 2 h with a heating rate of 5 °C min^{-1} in a muffle furnace. The final product was obtained after a sequence of grinding, washing with deionized water, and drying steps. The yield at one time was 2.5 g.

Material characterizations. A JEOL JSM-7100F scanning electron microscope (SEM) was used to obtain the surface morphology and corresponding elemental mappings. HAADF-STEM, SAED patterns, and EDS mappings were obtained from a 300 kV double corrected Titan G260-300 electron microscope. FIB/STEM imaging and the cross-sectional TEM specimen preparation were conducted on a FEI Helios Nanolab G3 UC FIB (Focused ion beam) operating at 2-30 kV. The electron beam Pt and ion beam Pt were firstly sputtered on Zn@ZSO foil surface one after another, and then a standard liftout procedure was used to directly prepare thin-section TEM specimen from bulk Zn@ZSO foil. ICP tests were carried out by a PerkinElmer Optima 4300DV spectrometer.

Electrochemical measurements. For preparation of KMO cathode electrode, the as-prepared KMO powder, Ketjen black, and polytetrafluoroethylene (PTFE) binder were mixed and ground with a mass ratio of 7 : 2 : 1. The mixture was then rolled into self-supporting film and cutted into several electrodes, which were finally dried at 80 °C for 12 h. The mass loading of the electrodes was ~8 mg cm^{-2}. Then, CR2032-type coin cells were assembled for electrochemical tests. Zn foil and Zn@ZSO foil were cutted into disc-shaped electrodes with a diameter of 12 mm. Glass fiber film (GF/D, Whatman) was used as the separator. 2 M $ZnSO_4$ and 2 M $ZnSO_4$ + 0.1 M $MnSO_4$ were used as electrolytes for symmetric and full cells, respectively.

Long-term cycling performance and rate performance of coin-type cells were tested by multichannel battery testing system (LAND CT2001A), and pouch cells were tested on Neware battery test systerm (CT-4008-5V6A-S1-F, Shenzhen, China). The voltage range for full cells was

0.8-1.9 V. The cyclic voltammetry (CV), electrochemical impedance spectroscopy (EIS), and chronoamperometry measurements were conducted by electrochemical workstation (EC-LAB).

Density functional theory (DFT) calculations. The present calculations were carried out by using the projector augmented wave (PAW)[2] method within the DFT as implemented in the Vienna ab initio simulation package (VASP).[3,4] The generalized gradient approximation (GGA) in the forms of Perdew-Burke-Ernzerhof (PBE) was used to treat the exchange-correlation energy.[5] DFT-D3 scheme was applied to account for the van der Waals interactions during the calculations.[6] The cutoff energy of 500 eV was chosen for wave functions expanded in plane wave basis. Slab models with 5~7 atomic layers and a vacuum slab of about 10 Å were constructed to simulate the (100) facet of Zn. The (400) and (131) facets of $ZnSiO_3$ were used during simulating. The adsorption energy (E_{ads}) was calculated by the following equation:

$$E_{ads} = E_{total} - E_{sub} - E_{Zn}$$

E_{total} represents the total energy of Zn(100), $ZnSiO_3$(400), and $ZnSiO_3$(131) substrates combined with zinc atom. Es_{ub} and E_{Zn} represent the energy of the substrate and the energy of zinc atom, respectively. The structures were visualized by utilization of VESTA software. For the Brillouin-zone sampling, 2×3×1, 2×3×1, and 1×1×1 of k-point was set for the structure relaxation of Zn(100), $ZnSiO_3$(400), and $ZnSiO_3$(131) substrate and increased to 6×6×6 for the electronic structure calculations of $ZnSiO_3$. Except for the bottom two atomic layers of the slab, all atoms were allowed to be fully relaxed while keeping the supercell boxes unchanged until the residual force per atom were less than 0.05 eV $Å^{-1}$. Ultrasoft pseudopotentials were used to describe the interaction of ionic core and valence electrons.

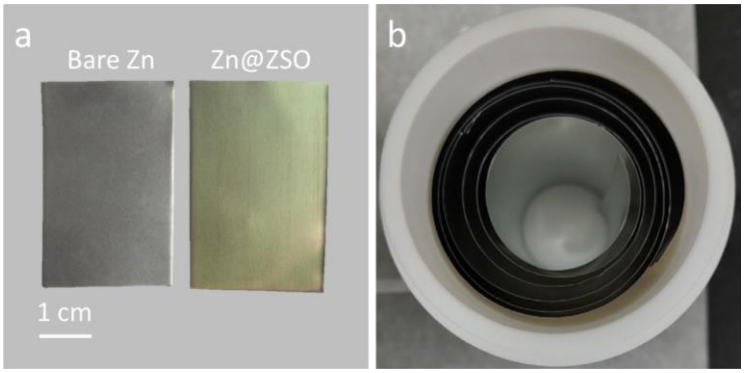

Figure S1. a) Digital photo of bare Zn and Zn@ZSO foils. b) Digital photo of rolled Zn foil in 500 mL reactor.

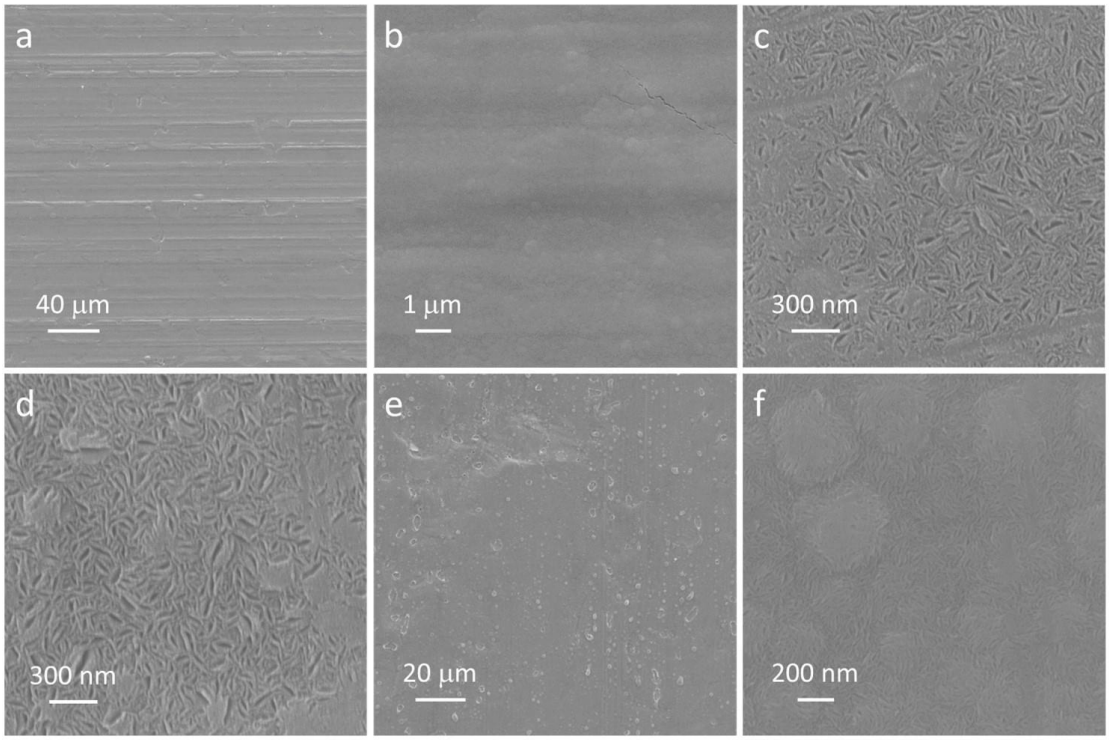

Figure S2. a,b) SEM images of Zn@ZSO. SEM images at c) edge and d) center of the large-area Zn@ZSO. e,f) SEM images of Zn@ZSO after ultrasound in ethanol at 40 kHz for 5 h.

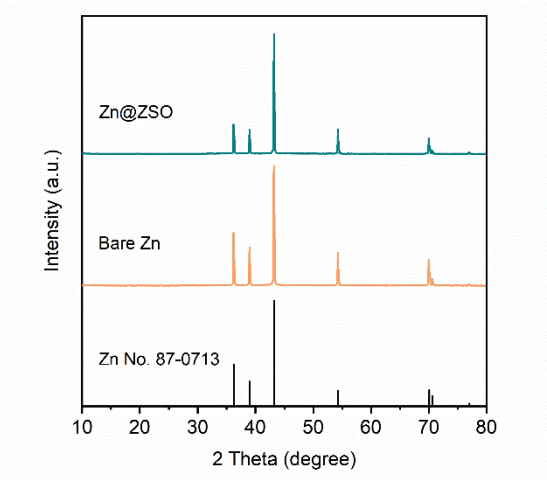

Figure S3. XRD patterns of Zn@ZSO and bare Zn.

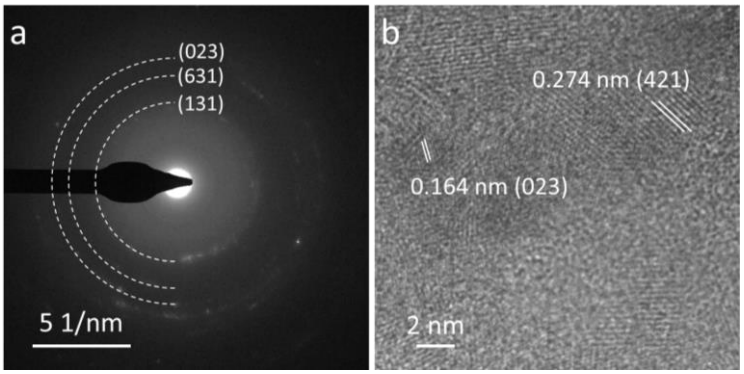

Figure S4. a) SAED pattern and b) HRTEM image of the ZSO layer.

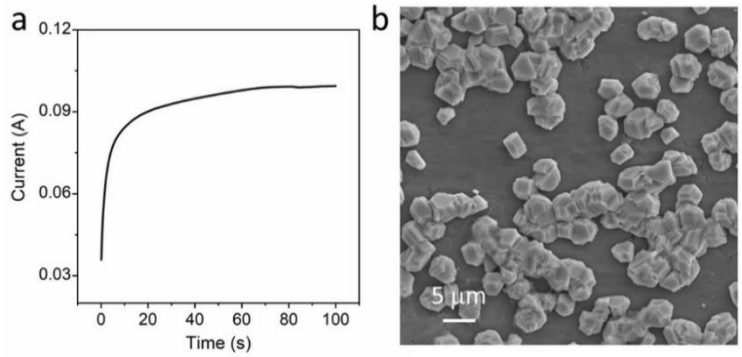

Figure S5. a) Amperometric i-t curve at −1.2 V vs. Hg/HgO in 2 M $ZnSO_4$ solution. b) SEM image of the prepared Ti@Zn.

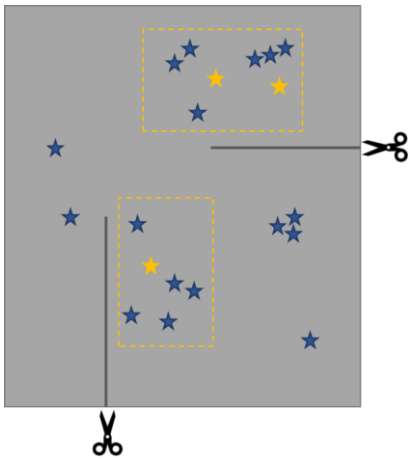

Figure S6. Schematic illustration of locating the Zn islands for observations.

The pentacles represent Zn islands on Ti foil, and the yellow ones are chosen for continuous observation. Macroscopically, the rough position on Ti foil was selected by shearing cracks. Microscopically, during the process of taking SEM images, Zn island around the crack was firstly chosen, then the other Zn islands around the chosen one were marked. In the next shooting, the same Zn island could be determined by looking for these specific locations and checking the distribution and morphology of the surrounding Zn islands.

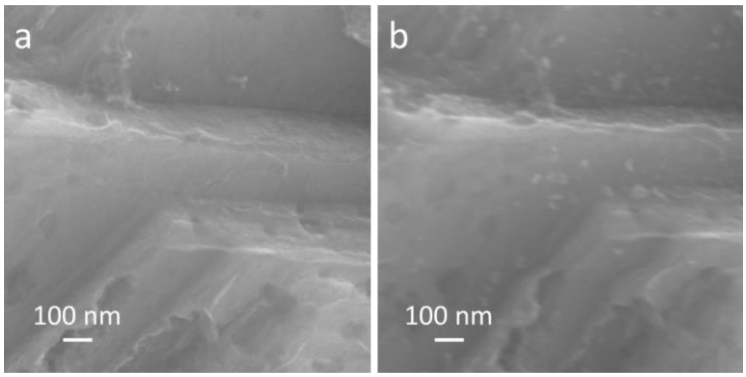

Figure S7. SEM images of the Zn island surface after reacting for a) 3 h and b) 8 h.

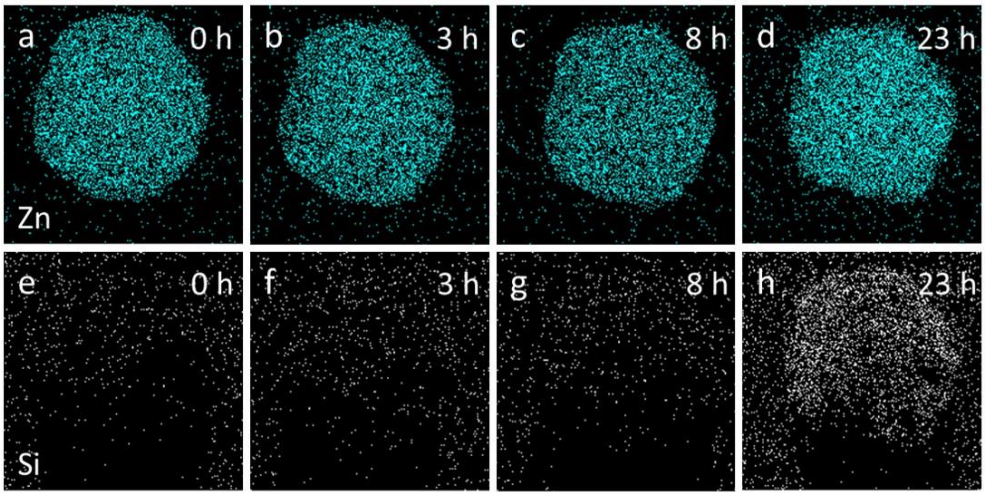

Figure S8. EDS mappings for a-d) Zn and e-h) Si elements of Zn island loaded on Ti foil initially and after reacting for 3, 8, and 23 h, respectively.

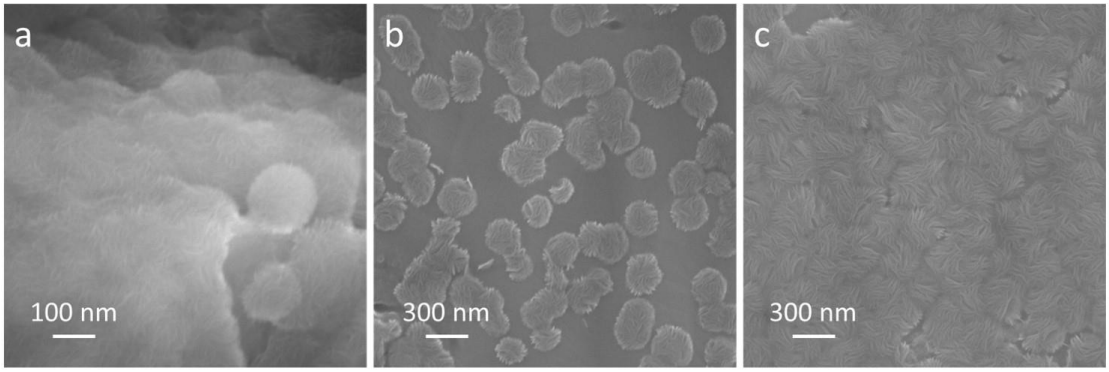

Figure S9. SEM images of a) Zn island surface after reaction for 23 h, b) Ti substrate surface after reaction for 23 h and c) Ti substrate surface after reaction for 29 h.

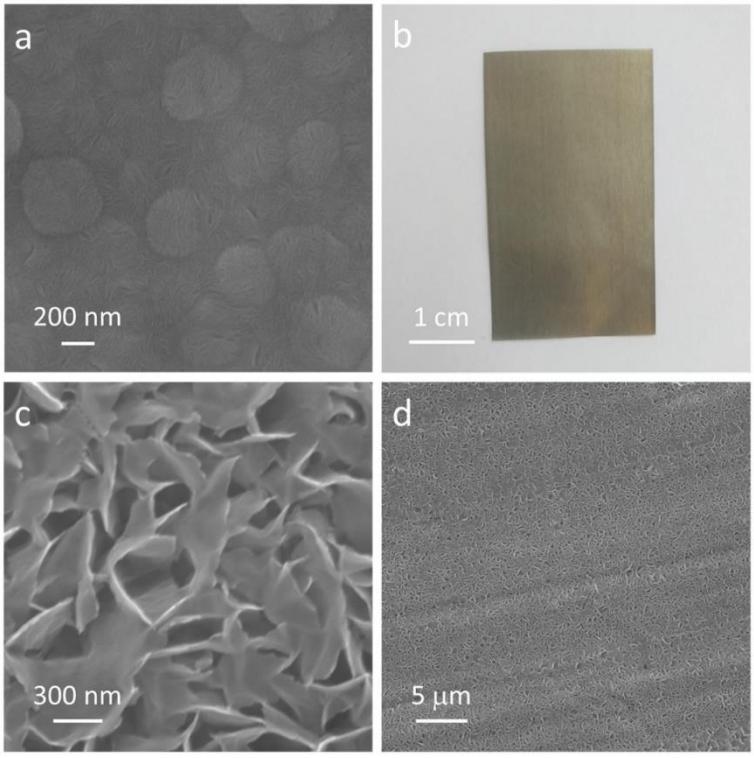

Figure S10. a) ZSO layer formed by using 50 nm SiO_2 as a raw material. b) Digital photo and c,d) SEM images of Zn@Zn-Ti-O composite foil.

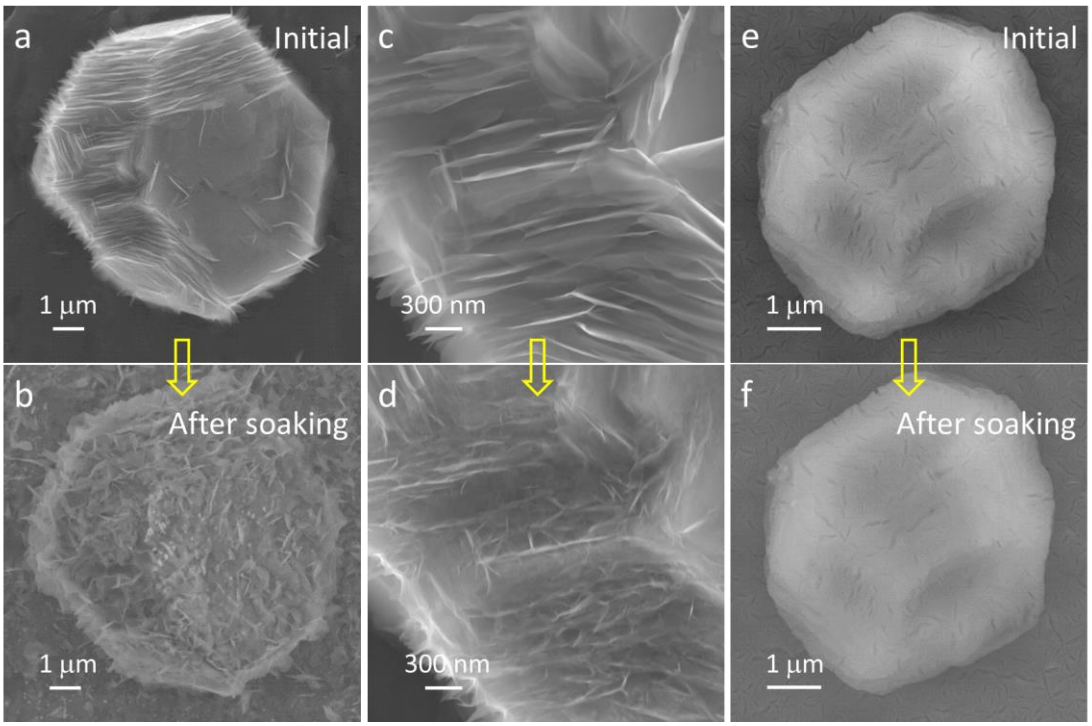

Figure S11. a,b) SEM images of Zn island initially and after soaking in 2 M $ZnSO_4$ for 3 h, respectively. c,d) SEM images of partial view of Zn island initially and after soaking in 2 M $ZnSO_4$

for 10 min, respectively. e,f) SEM images of Zn island@ZSO initially and after soaking in 2 M $ZnSO_4$ for 3 h, respectively.

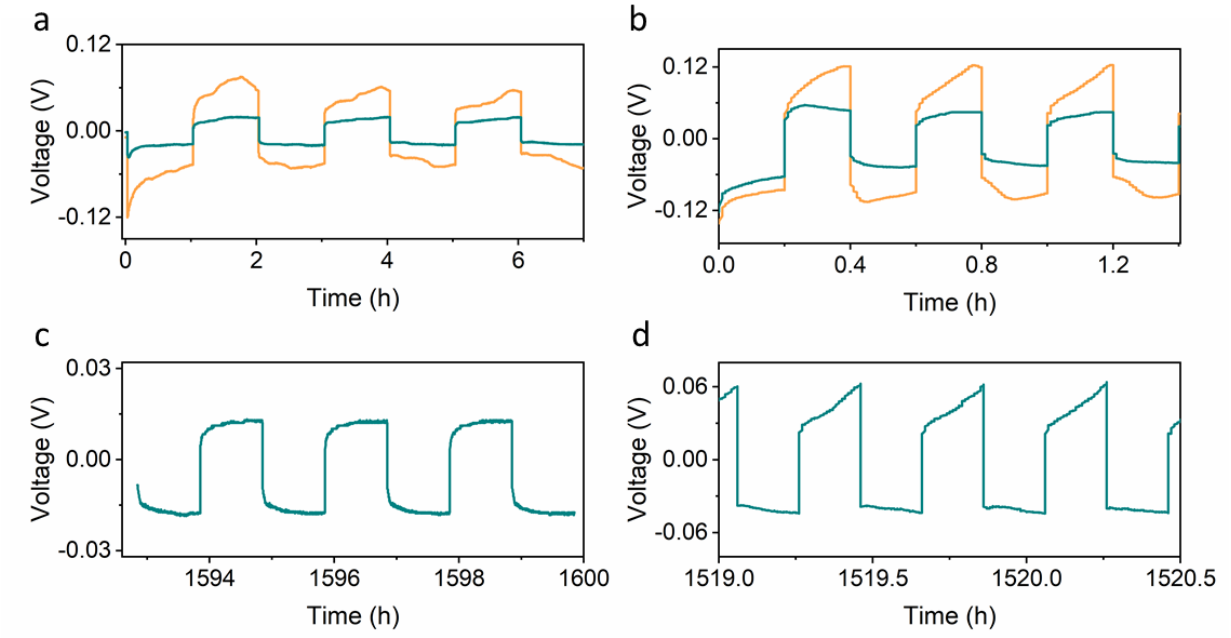

Figure S12. Voltage-time curves for 1-3 cycles of Zn@ZSO//Zn@ZSO and Zn//Zn symmetric cells at a) 1 and b) 5 mA cm^{-2}, and for the last three cycles of Zn@ZSO//Zn@ZSO symmetric cell at c) 1 and d) 5 mA cm^{-2}.

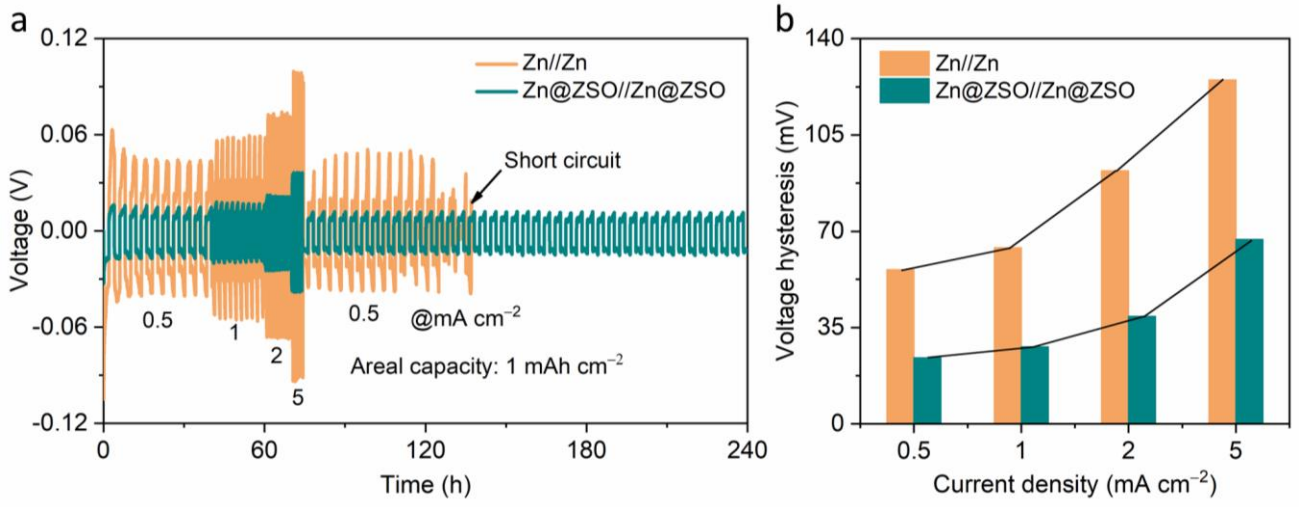

Figure S13. a) Rate performance and b) corresponding voltage hysteresis of Zn//Zn and Zn@ZSO//Zn@ZSO symmetric cells.

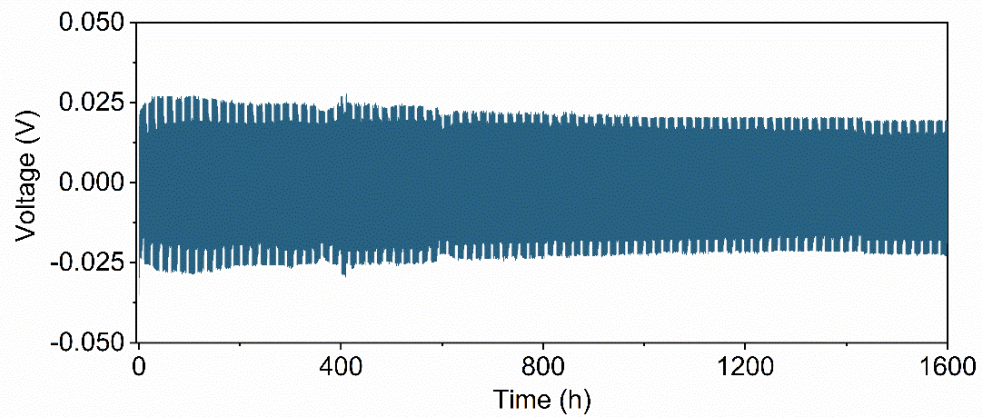

Figure S14. Galvanostatic cyling performance of Zn@Zn-Ti-O//Zn@Zn-Ti-O symmetric cell at 1 mA cm^{-2} with a capacity of 1 mAh cm^{-2}.

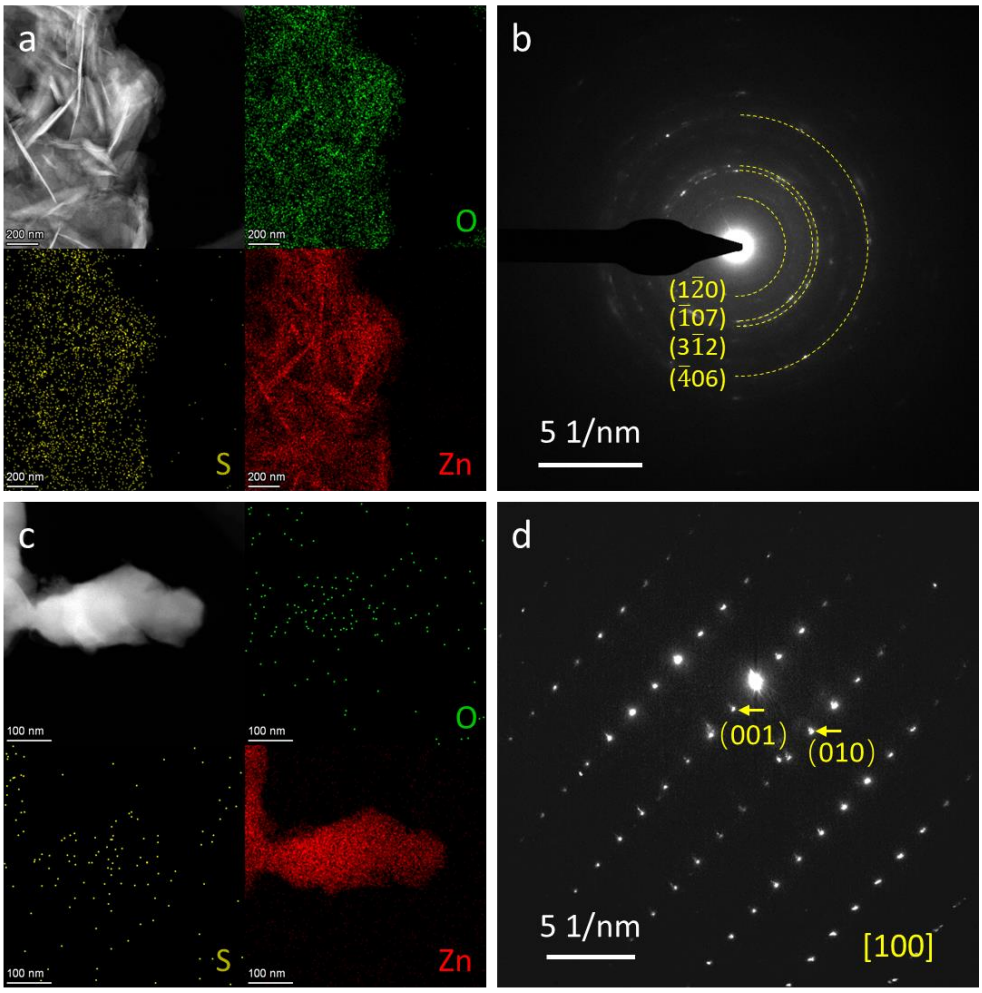

Figure S15. a) HAADF-STEM image and correponding elemental mappings, and b) SAED pattern of the appeared flake on Zn foil surface after plating for 40 min. c) HAADF-STEM image and

correponding elemental mappings, and d) SAED pattern of the dendrite on Zn foil surface after plating for 40 min.

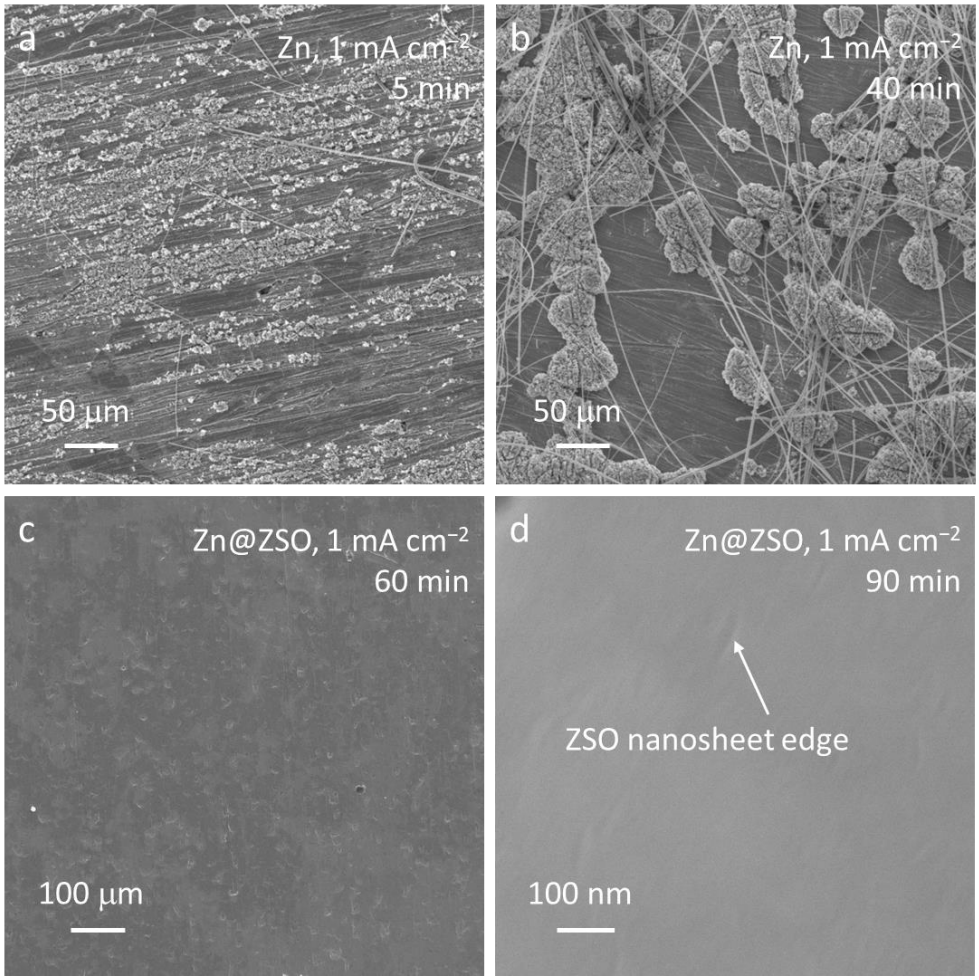

Figure S16. Low-magnification SEM images of Zn foil after plating for a) 5 min and b) 40 min. c) Low-magnification SEM image of Zn@ZSO after plating for 60 min. d) SEM image of Zn@ZSO after plating for 90 min. Current density: 1 mA cm^{-2}.

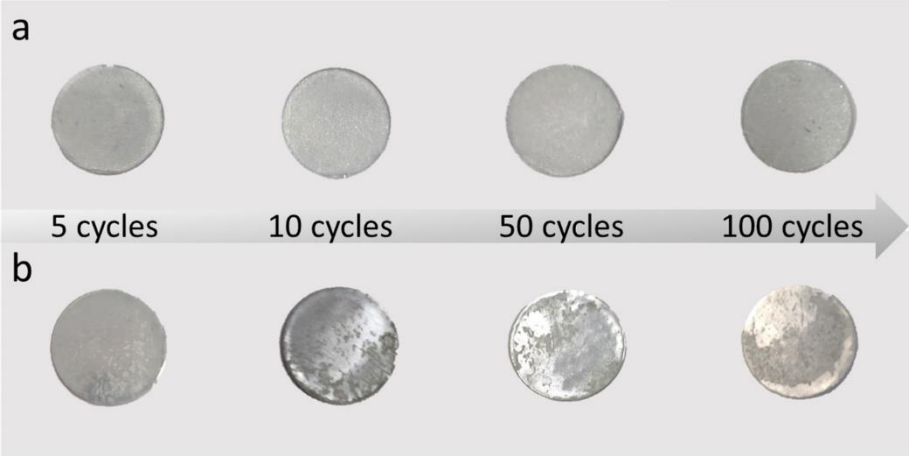

Figure S17. Digital photos of a) Zn@ZSO electrode and b) Zn electrode after 5, 10, 50, and 100 cycles at 5 mA cm^{-2} with an areal capacity of 1 mAh cm^{-2}.

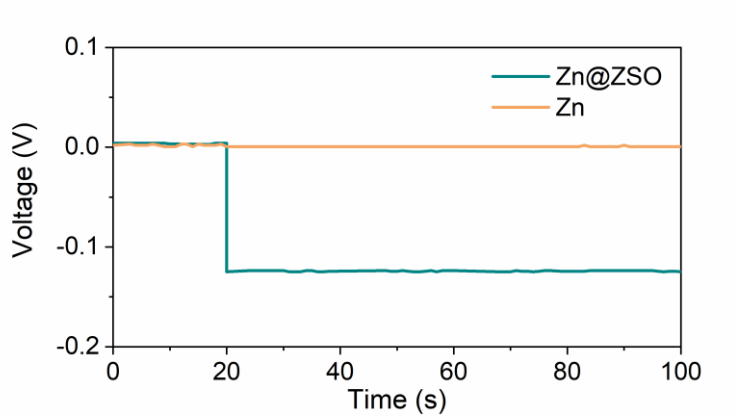

Figure S18. Voltage response curves of Zn and Zn@ZSO foils at a current of 5 mA after 20 s standing at open-circuit voltage.

To test the resistivity of ZSO layer, one side of Zn@ZSO was polished to expose the bright Zn, then the single-sided Zn@ZSO and pure Zn foil were sandwiched between two stainless steels. The voltage responses under a current of 5 mA were recorded after standing for 20 s at OCV, and the electrical resistivity was calculated based on the following equation[7]:

$$\rho = \frac{R * S}{L} = \frac{U * S}{I * L}$$

U refers to the average voltage (0.124 V), S refers to the area of the ZSO layer (1.131 cm^2), I refers to the current (5 mA), and L refers to the thickness of the ZSO layer (300 nm). Therefore, the calculated resistivity ρ is 9.18×10^5 Ω·cm.

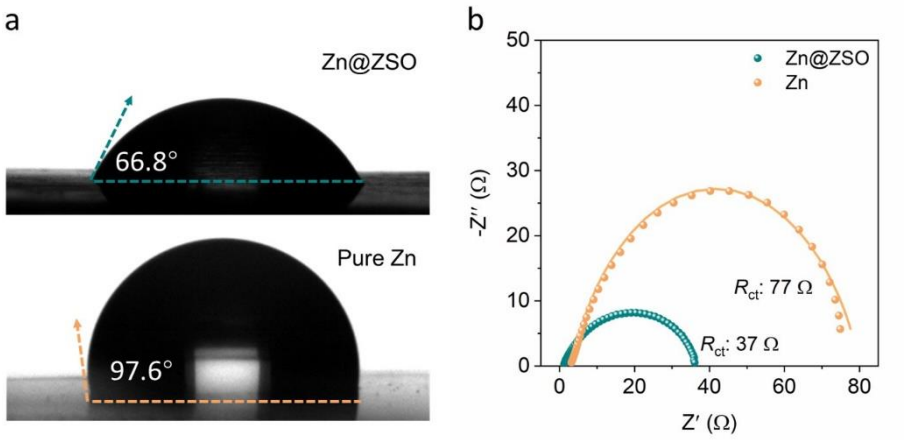

Figure S19. a) Contact angles of 2 M $ZnSO_4$ on Zn@ZSO and pure Zn foil. b) Nyquist plots of Zn//Zn and Zn@ZSO//Zn@ZSO symmetric cells.

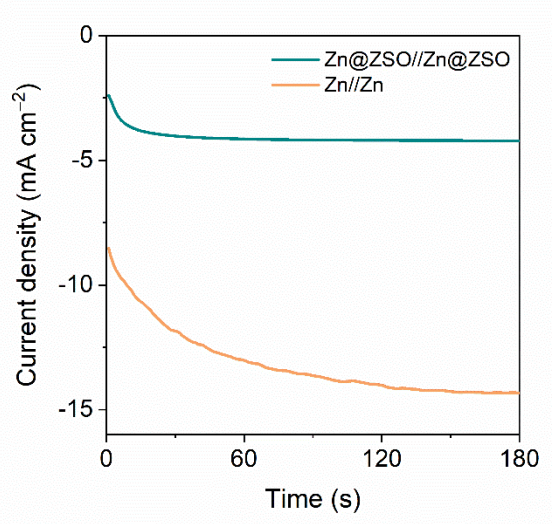

Figure S20. Chronoamperometry measurements of Zn//Zn and Zn@ZSO//Zn@ZSO symmetric cells at −150 mV.

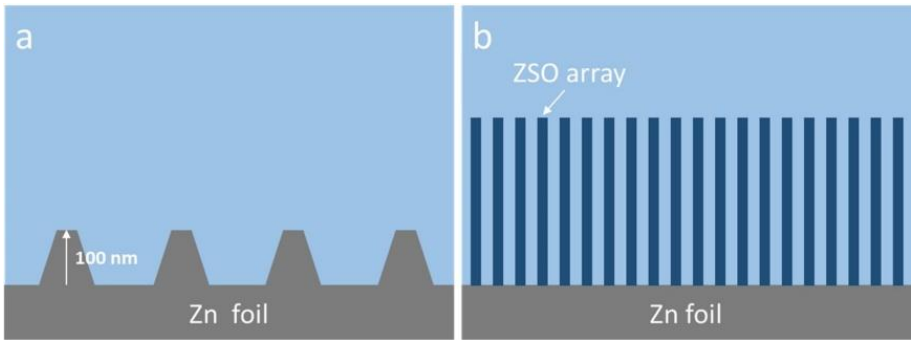

Figure S21. COMSOL models for a) Zn electrode and b) Zn@ZSO electrode.

To simulate the electric field distribution at the interface between anode and electrolyte, a simplified 2D model was established. The trapezoidal protrusions with a height of 100 nm represent the initial uneven nucleation of Zn (Figure S21a). The rectangles of 300 nm in height and 20 nm in width represent the ZSO nanosheets array (Figure S21b). The anode (the lower boundary of the model) was set as the ground (zero V). According to the Zn plating potential of symmetric cells, the potentials of cathode (the upper boundary of the model) were set as 55 mV for a), and 20 mV for b).

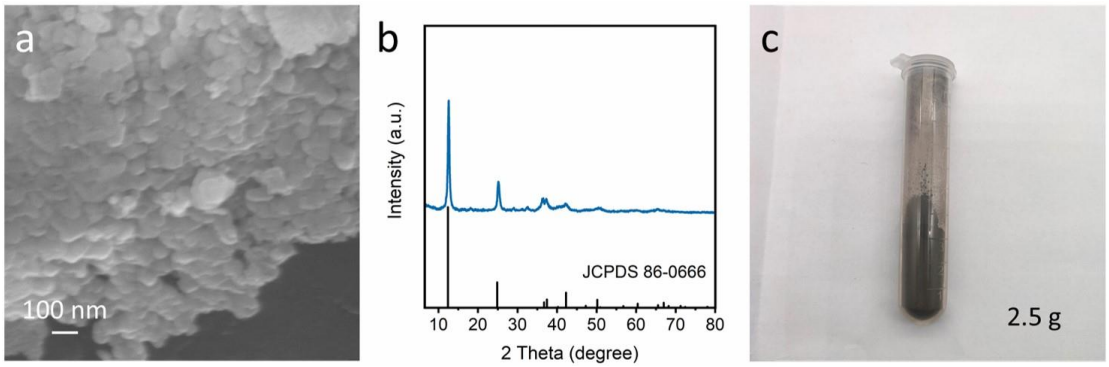

Figure S22. a) SEM image, b) XRD pattern, and c) digital photo of the prepared $K_{0.27}MnO_2 \cdot 0.54H_2O$ powder at one time.

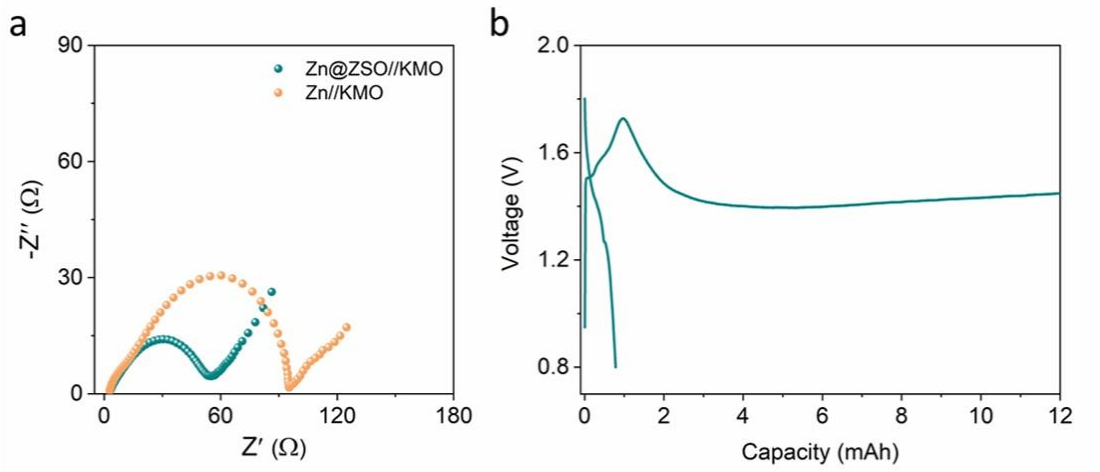

Figure S23. a) Nyquist plots of Zn@ZSO//KMO and Zn//KMO cells. b) Discharging and charging curves of Zn//KMO at the 123th cycle.

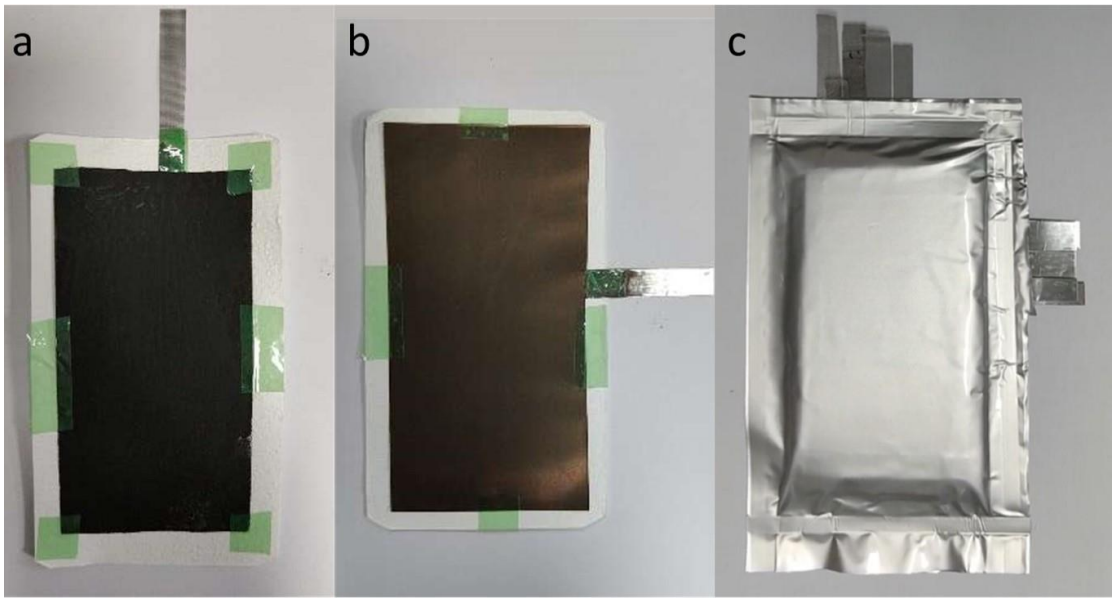

Figure S24. Digital photos of a) cathode film on Ti mesh, b) Zn@ZSO anode, and c) the assembled pouch cell with thickness of 5.5 mm. The white part in a) and b) is GF/A separator. Using GF/A as separator in the multi-layer pouch cell is to reduce its thickness and weight as much as possible. The exposed Ti meshes and polished Zn@ZSO were folded and rolled together to ensure good contact, respectively.

Table S1. Si/Zn atomic ratio in multiple areas.

Areas	Zn		Si		Si/Zn atomic ratio
	Atomic fraction (%)	Atomic error (%)	Atomic fraction (%)	Atomic error (%)	
#1	14.29	2.98	16.00	4.29	1.12
#2	14.27	3.21	15.10	4.24	1.06
#3	17.86	3.98	18.19	5.10	1.02
#4	17.38	3.90	20.62	5.73	1.18
#5	15.22	3.52	19.14	5.35	1.25
#6	16.40	3.59	15.35	4.40	0.93

Table S2. Comparison of Zn plating/stripping performance in this work with previous reports.

Interface layer (thickness)	Electrolyte	Current density (mA cm^{-2})	Areal capacity (mAh cm^{-2})	Voltage hysteresis (mV)	Cycle number
$Zn_3(PO_4)_2 \cdot 4H_2O$[8] (140 nm)	1 M $Zn(CF_3SO_3)_2$ + 25 mM $Zn(H_2PO_4)_2$	1	1	-	600
		5	1	-	550
$Zn_3(PO_4)_2/ZnF_2$[9] (-)	2 M $ZnSO_4$ + 0.05 M KPF_6	1	0.5	-	2200
$Zn_3(PO_4)_2$-ZnF_2-ZnS[10] (400-500 nm)	2 M $Zn(CF_3SO_3)_2$	1	0.5	108.8	2500
		5	2.5	158.9	600
ZnF_2[11] (9.3 μm)	2 M $ZnSO_4$	1	1	71.5	400
ZnS[7] (0.5 μm)	1 M $ZnSO_4$	2	2	98	550
ZnO-3D[12] (-)	2 M $ZnSO_4$ + 0.1 M $MnSO_4$	5	1.25	86	1000
PAN/$Zn(TfO)_2$[13] (11 μm)	2 M $Zn(CF_3SO_3)_2$	1	1	150	572
$NaTi_2(PO_4)_3$[14] (20-25 μm)	2 M $ZnSO_4$	1	1	30-50	130
DIP D COF flm[15] (70 nm)	2 M $ZnSO_4$	1	1	36	210
ALD-Al_2O_3[16] (10 nm)	3 M $Zn(CF_3SO_3)_2$	1	1	36.5	250
ZrO_2[17] (4 μm)	2 M $ZnSO_4$	0.25	0.125	50	3800
Poled $BaTiO_3$[18] (15 μm)	1 M $ZnSO_4$ + 0.1 M $MnSO_4$	1	1	60-100	2050
F-TiO_2[19] (20 μm)	1 M $ZnSO_4$	1	1	40	230
$ZnSiO_3$ (this work) (300 nm)	**2 M $ZnSO_4$**	**1**	**1**	**21**	**800**
		5	**1**	**67**	**3800**

Note. Voltage hysteresis was unified as the gap between plating plateau and stripping plateau. PAN: Polyacrylonitrile. Zn(TfO)2: zinc trifluoromethanesulfonate. COF: Covalent Organic Framework.

Table S3. Comparison of coin-type full cell performance in this work with previous reports.

Interface layer	Cathode and mass loading (mg cm^{-2})	Electrolyte	Specific capacity (mAh g^{-1})	Cycle number*	Cumulative capacity (mAh cm^{-2})
$ZnSiO_3$ (this work)	$K_{0.27}MnO_2 \cdot 0.54H_2O$ **8**	2 M $ZnSO_4$ + 0.1 M $MnSO_4$	171.5	400/123*	548.9
ZnS[7]	MnO_2 **0.8**	1 M $ZnSO_4$ + 0.1 M $MnSO_4$	110.2	2500/1000*	220.4
$Zn_3(PO_4)_2/ZnF_2$[9]	MnO_2/CNT **1**	2 M $ZnSO_4$ + 0.1 M $MnSO_4$	125-150	600/350	75-90
ZnF_2[11]	α-MnO_2 **1.2-1.5**	2 M $ZnSO_4$ + 0.1 M $MnSO_4$	234.8	250/250	70.4-88.0
P(VDF-TrFE)[20]	α-MnO_2 **1**	2 M $ZnSO_4$ + 0.1 M $MnSO_4$	163	300/300	48.9
PDMS/TiO_{2-x}[21]	α-MnO_2 **1.5**	1 M or 3 M $ZnSO_4$	179	400/400	107.4
$Zn_{0.73}Al_{0.27}$[22]	MnO_2 **2**	2 M $ZnSO_4$ + 0.1 M $MnSO_4$	140-200	1000/1000	280-400
$NaTi_2(PO_4)_3$[14]	MnO_2/CNT **1-2**	2 M $ZnSO_4$ + 0.2 M $MnSO_4$	128	600/600	76.8-153.6
ZrO_2[17]	V_2O_5 **1**	2 M $ZnSO_4$	70	3000/1145*	210
DIP D COF[15]	δ-MnO_2 **2**	2 M $ZnSO_4$ + 0.2 M $MnSO_4$	220-250	300/300	132-150
PVB[23]	MnO_2/CC **1.1**	1 M $ZnSO_4$ + 0.1 M $MnSO_4$	120-140	1500/1500	198-231
MXene[24]	α-MnO_2 **1**	2 M $ZnSO_4$	205.5	500/500	102.7
ZnF_2-Cu[25]	V_2O_5 **1.5**	2 M $ZnSO_4$	100-150	2000/372*	300-400
MXene/chitosan[26]	MnO_2 **1.05**	2 M $ZnSO_4$ + 0.1 M $MnSO_4$	150-180	400/200	63-75.6
$Zn_3(PO_4)_2 \cdot 4H_2O$[8]	V_2O_5 **5**	1 M $Zn(CF_3SO_3)_2$ + 25 mM $Zn(H_2PO_4)_2$	100-125	1000/200*	500-625
S-BN[27]	$Na_2V_6O_{16} \cdot 1.63H_2O$ **1**	2 M $ZnSO_4$	150-175	1200/1200	180-210

Note. Cumulative capacity is the product of discharge specific capacity, cycle number and mass loading, and this value in this work is obtained by the sum of areal capacity in every cycle. For other works, the given values of reversible specific capacity or their main distribution range are used for calculation.

Cycle number* refers to the cycles numbers of experimental group (left) and control group (right, bare Zn as an anode).

* represents that the cell with bare Zn anode is in a failure by the given cycle number value.

P(VDF-TrFE): poly(vinylidene fluoride-trifluoroethylene. PDMS: Polydimethylsiloxane. PVB: Polyvinyl butyral. S-BN: Sulfonate group modified boron nitride nanosheets.

Reference

[1] Y. Jiao, L. Kang, J. Berry-Gair, K. McColl, J. Li, H. Dong, H. Jiang, R. Wang, F. Cora, D. J. Brett, *J. Mater. Chem. A* **2020**, *8*, 22075.

[2] G. Kresse, D. Joubert, *Phys. Rev. B* **1999**, *59*, 1758.

[3] G. Kresse, J. Furthmüller, *Phys. Rev. B* **1996**, *54*, 11169.

[4] G. Kresse, J. Furthmüller, *Comput. Mater. Sci.* **1996**, *6*, 15.

[5] J. P. Perdew, K. Burke, M. Ernzerhof, *Phys. Rev. Lett.* **1996**, *77*, 3865.

[6] S. Grimme, S. Ehrlich, L. Goerigk, *J. Comput. Chem.* **2011**, *32*, 1456.

[7] J. Hao, B. Li, X. Li, X. Zeng, S. Zhang, F. Yang, S. Liu, D. Li, C. Wu, Z. Guo, *Adv. Mater.* **2020**, *32*, 2003021.

[8] X. Zeng, J. Mao, J. Hao, J. Liu, S. Liu, Z. Wang, Y. Wang, S. Zhang, T. Zheng, J. Liu, *Adv. Mater.* **2021**, *33*, 2007416.

[9] Y. Chu, S. Zhang, S. Wu, Z. Hu, G. Cui, J. Luo, *Energy Environ. Sci.* **2021**, *14*, 3609.

[10] S. Di, X. Nie, G. Ma, W. Yuan, Y. Wang, Y. Liu, S. Shen, N. Zhang, *Energy Storage Mater.* **2021**, *43*, 375.

[11] Y. Yang, C. Liu, Z. Lv, H. Yang, Y. Zhang, M. Ye, L. Chen, J. Zhao, C. Li, *Adv. Mater.* **2021**, *33*, 2007388.

[12] X. Xie, S. Liang, J. Gao, S. Guo, J. Guo, C. Wang, G. Xu, X. Wu, G. Chen, J. Zhou, *Energy Environ. Sci.* **2020**, *13*, 503.

[13] P. Chen, X. Yuan, Y. Xia, Y. Zhang, L. Fu, L. Liu, N. Yu, Q. Huang, B. Wang, X. Hu, *Adv. Sci.* **2021**, *8*, 2100309.

[14] M. Liu, J. Cai, H. Ao, Z. Hou, Y. Zhu, Y. Qian, *Adv. Funct. Mater.* **2020**, *30*, 2004885.

[15] J. Park, M.-J. Kwak, C. Hwang, K.-N. Kang, N. Liu, J.-H. Jang, B. A. Grzybowski, *Adv. Mater.* **2021**, *33*, 2101726.

[16] H. He, H. Tong, X. Song, X. Song, J. Liu, *J. Mater. Chem. A* **2020**, *8*, 7836.

[17] P. Liang, J. Yi, X. Liu, K. Wu, Z. Wang, J. Cui, Y. Liu, Y. Wang, Y. Xia, J. Zhang, *Adv. Funct. Mater.* **2020**, *30*, 1908528.

[18] P. Zou, R. Zhang, L. Yao, J. Qin, K. Kisslinger, H. Zhuang, H. L. Xin, *Adv. Energy Mater.* **2021**, *11*, 2100982.
[19] Q. Zhang, J. Luan, X. Huang, Q. Wang, D. Sun, Y. Tang, X. Ji, H. Wang, *Nat. Commun.* **2020**, *11*, 1.
[20] Y. Wang, T. Guo, J. Yin, Z. Tian, Y. Ma, Z. Liu, Y. Zhu, H. N. Alshareef, *Adv. Mater.* **2022**, *34*, 2106937.
[21] Z. Guo, L. Fan, C. Zhao, A. Chen, N. Liu, Y. Zhang, N. Zhang, *Adv. Mater.* **2022**, *34*, 2105133.
[22] J. Zheng, Z. Huang, Y. Zeng, W. Liu, B. Wei, Z. Qi, Z. Wang, C. Xia, H. Liang, *Nano Lett.* **2022**, *22*, 1017.
[23] J. Hao, X. Li, S. Zhang, F. Yang, X. Zeng, S. Zhang, G. Bo, C. Wang, Z. Guo, *Adv. Funct. Mater.* **2020**, *30*, 2001263.
[24] N. Zhang, S. Huang, Z. Suan, J. Zhu, Z. Zhao, Z. Niu, *Angew. Chem., Int. Ed.* **2021**, *60*, 2861.
[25] Y. Mu, T. Zhou, D. Li, W. Liu, P. Jiang, L. Chen, H. Zhou, G. Ge, *Chem. Eng. J.* **2022**, *430*, 132839.
[26] L. Tan, C. Wei, Y. Zhang, Y. An, S. Xiong, J. Feng, *Chem. Eng. J.* **2021**, *431*, 134277.
[27] M. Qiu, H. Jia, C. Lan, H. Liu, S. Fu, *Energy Storage Mater.* **2022**, *45*, 1175.